

# Electro-conductive porous ceramics prepared by chemical vapor infiltration of TiN

Yoshimi Ohzawa · Xingun Cheng · Takashi Achiha ·  
Tsuyoshi Nakajima · Henri Groult

Received: 6 September 2007 / Accepted: 6 February 2008 / Published online: 28 February 2008  
© Springer Science+Business Media, LLC 2008

**Abstract** Using pressure-pulsed chemical vapor infiltration (PCVI) method, TiN was partially infiltrated at 850 °C from gas system of TiCl<sub>4</sub> (1%)–N<sub>2</sub> (10%)–H<sub>2</sub> into the highly porous carbon substrates prepared by the carbonization of cotton-wool, filter paper, and wood at 1,000 °C in Ar for 4 h. After 10,000 pulses of PCVI, electro-conductive porous ceramics having the three-dimensionally continuous current paths were obtained, which had the porosity of 80% and more, the resistivity of 10<sup>-5</sup>–10<sup>-6</sup> Ω m, and the average pore sizes of 10–40 μm. The geometric surface area per unit volume of the sample was higher than that of the conventional foil-type current collector for lithium-ion battery. The surface area showed the highest value for the sample obtained from carbonized wood substrate.

## Introduction

Chemical vapor infiltration (CVI) has received attention as a preparation process for the fiber- or particle-reinforced composites. In this process, the source gases are flowed through the fibrous or particulate preforms at a high temperature, during which specific material is deposited as a matrix between the fibers or particles [1, 2]. In the past few decades, three main methods were developed; isothermal

and isobaric CVI (ICVI) [3], forced CVI (FCVI) [4], and pressure-pulsed CVI (PCVI) [5–8]. In the PCVI process, the following steps are repeated; evacuation of the reaction vessel, instantaneous introduction of the source gas, and holding to allow deposition. Compared with the conventional CVD process, PCVI process allows homogeneous infiltration of matrix through the thickness of the preforms under suitable conditions because of rapid penetration of the source gas throughout the preform without pre-heating [9, 10].

Recently, PCVI method has been applied to synthesize the porous ceramics, for example, the porous SiC foams prepared by partial densification with SiC matrix into the biologically derived porous preforms such as the carbonized wood, cotton, and paper [11, 12]. In similar process, if electro-conductive materials such as TiN and TiC are partially infiltrated instead of SiC matrix, highly porous electro-conductive ceramics would be obtained. Utilizing these conductive porous substrates as the conductive fillers and/or current collectors for the secondary batteries such as Ni–H and Lithium-ion battery, it is expected that the inner resistance of the battery is reduced because the three-dimensionally continuous current paths are formed in the active material layer of the electrodes. The formation of current paths could decrease the organic binder and additional conductive filler added to assist the construction of conduction network. The reductions of these additives and inner resistance would increase the energy and/or power density of the battery.

In this study, the new preparation process of the electro-conductive porous ceramics was investigated using PCVI of TiN into highly porous carbon substrates prepared by the carbonization of cotton, paper, and wood. And the properties on the current collector were estimated for the lithium-ion secondary batteries.

Y. Ohzawa (✉) · X. Cheng · T. Achiha · T. Nakajima  
Department of Applied Chemistry, Aichi Institute of  
Technology, Yachigusa 1247, Yakusa-cho, Toyota 470-0392,  
Japan  
e-mail: ohzawa@aitech.ac.jp

H. Groult  
Laboratory of Electrolytes and Electrochemistry, University  
of Pierre and Marie Curie, Paris Cedex 05 75252, France

**Experimental**

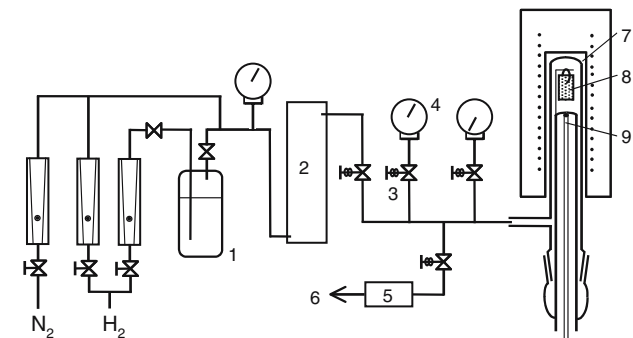
Highly porous carbon substrates were prepared as follows. Commercial cotton-cloth, cotton-wool, filter paper, and wood (cedar) were put between carbon plates, carbonized at 1,000 °C in Ar for 4 h, and cut to 10 × 15 mm<sup>2</sup>. Table 1 shows the dimension and the initial porosity (ε<sub>0</sub>) of each substrate. The ε<sub>0</sub> of the carbonized substrate was calculated by dividing the apparent density of porous substrate by carbon density of 1.8 g cm<sup>-1</sup>, where apparent density was estimated from the mass and volume of the substrate.

Figure 1 shows the apparatus of PCVI for TiN. The source gas mixture of TiCl<sub>4</sub> (1%)–N<sub>2</sub> (10%)–H<sub>2</sub> was allowed to flow into a reservoir. It was instantaneously introduced (within 0.1 s) into the reaction vessel up to 0.1 MPa, and pressure was held under same condition to allow matrix deposition (holding time, 1.5 s). Then, the gas was evacuated to below 0.7 kPa within 1.5 s. This cycle of the sequential steps was defined as one pulse, and it was repeated to the desired number of times. The CVI temperature was kept at 850 °C.

The filling ratio (*F*<sub>TiN</sub>) was defined as the fraction of infiltrated TiN matrix volume (*V*<sub>TiN</sub>) per initial pore volume in the substrate (*V*<sub>pore</sub>), where *V*<sub>TiN</sub> and *V*<sub>pore</sub> were estimated from the weight increase, the substrate volume (*V*<sub>sub</sub>), and the initial porosity (ε<sub>0</sub>) of the substrate.

**Table 1** Dimension and initial porosity data of porous carbon-substrates

Substrate	Dimension (mm)	Porosity, ε <sub>0</sub> (%)
Cotton-cloth	10 × 15 × 0.1	85–87
Cotton-wool	10 × 15 × 1.0	95–98
Filter paper	10 × 15 × 0.8	92–94
Wood	10 × 15 × 0.5	88–90



**Fig. 1** Apparatus for pressure-pulsed chemical vapor infiltration of TiN. 1, TiCl<sub>4</sub> saturator; 2, reservoir; 3, electromagnetic valve; 4, pressure gauge; 5, vacuum tank; 6, to vacuum pump; 7, furnace; 8, substrate; 9, thermocouple

$$F_{TiN} = V_{TiN}/V_{pore} = V_{TiN}/(\epsilon_0 V_{sub}) \tag{1}$$

Residual porosity (ε) of the sample was calculated from the following equation:

$$\epsilon = \epsilon_0 [1 - (V_{TiN}/V_{pore})] \tag{2}$$

In the calculation, the densities of TiN deposits and substrate carbon were assumed to be 5.4 and 1.8 g cm<sup>-3</sup>, respectively.

The average pore size was determined by the bubble-point method according to ASTM F 316. In this method, the air pressures and the flow rates are measured for both dry and fluid-wet sample (undecane was used for the fluid in the present measurement). The air flows through the wet sample when the applied air pressure exceeds the capillary attraction of the fluid into the pore, where the pressure is inversely proportional to the pore size. By comparing the air flow rates of both the wet and the dry samples at the same pressure, the volume percentage of the pores that air passes through can be calculated, and the average pore size is determined by a pressure at which the wet sample flow is half of the dry sample flow. Geometric surface area (*S*<sub>v</sub>) was calculated using the Kozeny–Carman equation from the gas-permeability (i.e. pressure drop, Δ*P*) measured on the bubble-point method;

$$\Delta P = k \mu L u \epsilon^{-3} S_v^2 \tag{7}$$

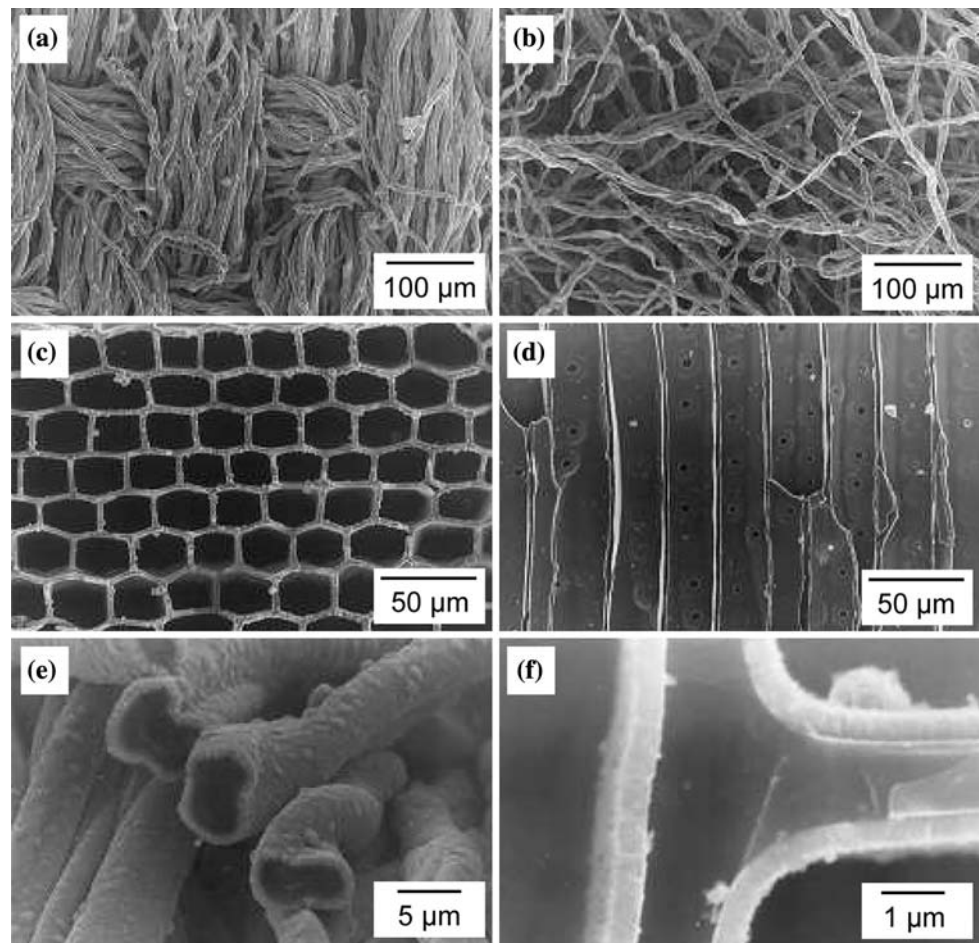
where *k*, constant decided by experiment (=5); μ, viscosity of gas (kg m<sup>-1</sup> s<sup>-1</sup>); *L*, length of packed bed (m); *u*, superficial velocity of gas (m s<sup>-1</sup>).

Specific resistance was measured by four-terminal method at room temperature, in which four Cu wires of 0.8 mm in diameter were attached on the plate-like sample using Ag paste. JSM-820 (JEOL) was used for the scanning electron microscopy (SEM). The composition of the deposited TiN was estimated by X-ray photoelectron spectroscopy (XPS, Shimadzu, ESCA 3400 with MgKα radiation).

**Results and discussion**

Figure 2 shows the SEM images of the electro-conductive porous ceramics obtained after 10,000 pulses of PCVI, where the samples were prepared from the carbonized cotton-cloth {photograph (a)}, cotton-wool {(b) and (e)}, and wood substrates {(c), (d), and (f)}. From low-magnification photographs (a) and (b), it can be observed that the prepared samples have the continuous fibers retaining the fibrous structure of the carbon substrates and that the TiN-coated fibers connect with each other. The fibers in the sample obtained from the carbonized cloth {photograph (a)} are arranged with a regular orientation reflecting the

**Fig. 2** SEM images of the electro-conductive porous ceramics obtained after 10000 pulses of PCVI with TiN into the carbonized cotton-cloth {photograph (a)}, cotton-wool {(b) and (e)}, and wood {(c), (d), and (f)} substrates



two-dimensionally woven structure of the substrate. Carbonized wool/TiN sample {photograph (b)} have a relatively random orientation. On the other hand, it can be observed from photograph (c) and (d) that the carbonized wood/TiN sample has a honeycomb-shaped cellular structure and the pores with the cross-section of rectangle, penetrating through the substrate. From these observations, it is considered that the present samples have the three-dimensionally continuous current paths in the porous bodies. Photographs (e) and (f) show high-magnification images of the cross-section of the samples (b) and (c), respectively. It can be found that TiN films with a thickness of 0.5–1  $\mu\text{m}$  deposit around the carbonized fibers of about 6  $\mu\text{m}$  in diameter {photograph (e)} or on the cell walls of the carbonized wood {photograph (f)}. It appears that TiN films adhere tightly to the carbonized fibers or the cell walls.

In Fig. 3, the change of the TiN-filling ratio ( $F_{\text{TiN}}$ ) with number of pulses in PCVI treatment was shown for the samples obtained from the carbonized wool and wood substrates.  $F_{\text{TiN}}$  for each sample increases linearly up to 20,000 pulses. The increasing rate of  $F_{\text{TiN}}$  for the carbonized wood/TiN sample is higher than that for the wool/TiN

sample, reflecting the difference in initial porosity ( $\varepsilon_0$ ) of the carbon substrate. The area of the carbon surface on which TiN film can be deposited increases with the carbon volume fraction, which increases with the decrease of  $\varepsilon_0$ . Therefore, high rate infiltration is achieved for the substrate having the lower  $\varepsilon_0$ , assuming that the growth rate of TiN film is constant.

Figure 4 shows the change of the apparent resistivity of each sample ( $R_S$ ) obtained from the carbonized wool or wood substrates with number of pulses. For both samples,  $R_S$  is rapidly lowered at the early stage of TiN infiltration, and then gradually decreased with number of pulses.  $R_S$  of the carbonized wool/TiN sample is higher than that of the wood/TiN sample because the volume fraction of carbon and TiN for the former is lower than that for the latter.  $R_S$  of the present sample is roughly estimated from the specific resistance of carbon ( $\rho_C$ ) and TiN ( $\rho_{\text{TiN}}$ );

$$\frac{1}{R_S} = \frac{V_C}{\rho_C V_S} + \frac{V_{\text{TiN}}}{\rho_{\text{TiN}} V_S} \quad (3)$$

where  $V_C$ ,  $V_{\text{TiN}}$ , and  $V_S$  are volume of carbon, TiN, and sample, respectively. In Eq. 3,  $V_C/V_S$  and  $V_{\text{TiN}}/V_S$  indicate the volume fraction of substrate carbon and TiN,

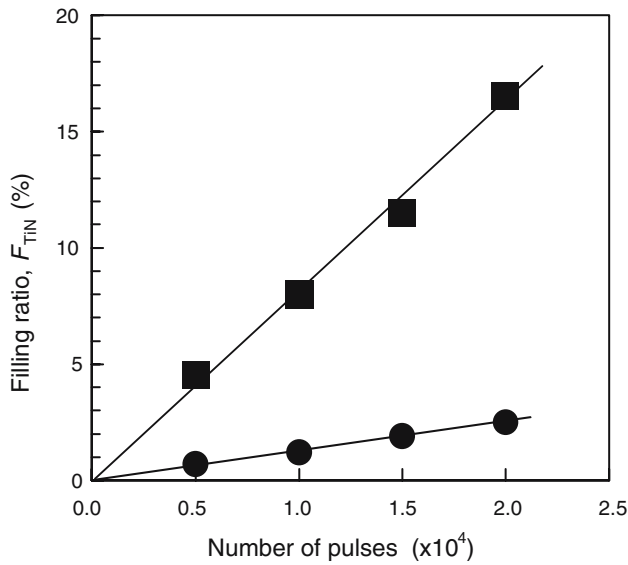


**Fig. 3** Change of TiN-filling ratio ( $F_{TiN}$ ) with number of pulses for PCVI treatment into the carbonized wool (●) and wood (■) substrates

respectively. The  $\rho_{TiN}$  value is around  $4 \times 10^{-7} \Omega m$  [13], and  $\rho_C$  for low crystalline carbon is approximately  $10^3$  times higher than  $\rho_{TiN}$ . Therefore, electro conductivity of substrate carbon can be ignored, then Eq. 4 is obtained from Eq. 3:

$$R_S = \frac{\rho_{TiN} V_S}{V_{TiN}} \quad (4)$$

Regarding  $V_S$  as  $V_{sub}$ , Eq. 5 is derived from Eqs. 1 and 3:

$$R_S = \frac{\rho_{TiN}}{\epsilon_0 F_{TiN}} \quad (5)$$

The dashed lines in Fig. 4 show  $R_S$  calculated by Eq. 5 using  $F_{TiN}$  in Fig. 3. It is considered that the change of

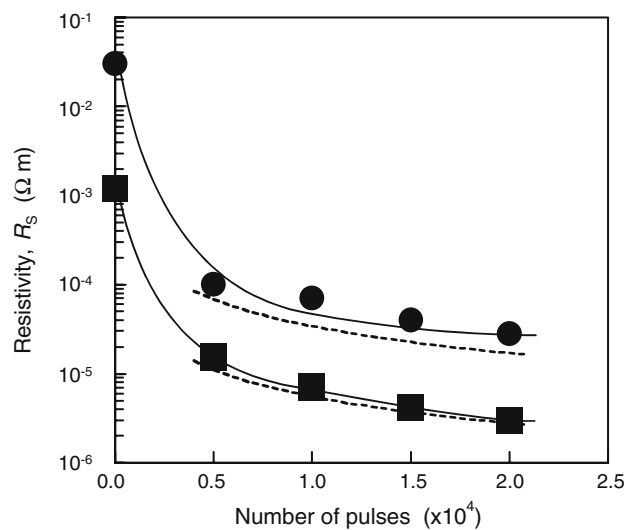


**Fig. 4** Change of apparent resistivity ( $R_S$ ) with number of pulses for PCVI treatment into the carbonized wool (●) and wood (■) substrates

calculated  $R_S$  agrees qualitatively with the experimental results.

In Fig. 5, the typical XPS spectra of the porous TiN-coated ceramics. The N 1 s spectrum is observed at around 395.7 eV, and Ti 2p 1/2 and Ti 2p 3/2 peaks are at around 464.0 and 458.2 eV, respectively. The atomic ratio (N/Ti) of the deposited TiN film was 1.1, calculated from the peak area of XPS. The resistivity of TiN depends strongly on its composition. TiN composition could be varied by the CVD condition such as temperature, gas ratio of  $N_2/TiCl_4$ , and partial pressure of  $TiCl_4$ . In general, the stoichiometric TiN could be deposited at temperature above 1,000 °C. In CVI process, however, low temperature condition is required to achieve the uniform infiltration of matrix over the thickness of porous substrate. The temperature elevation leads to the increase of reaction rate, resulting in the film formation only on the external surface of porous substrate in early stage of PCVI treatment. Film on the external surface prevents the source gas penetration into the inner part of the porous substrate, causing to the decrease in the thickness of TiN layer toward the center of substrate in depth.

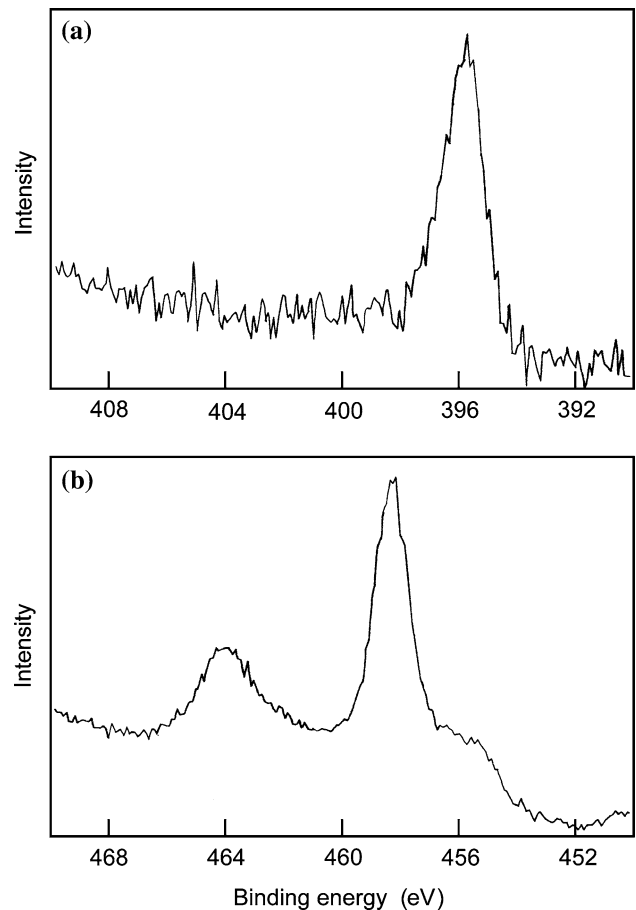


**Fig. 5** N 1 s (a) and Ti 2p (b) spectra in X-ray photoelectron spectroscopy of porous ceramics obtained after 10,000 pulses of PCVI with TiN into carbonized wood substrate

**Table 2** Specific properties of porous TiN-based ceramics

	Sample	Porosity (%)	Resistivity ( $\Omega$ m)	Average pore size ( $\mu\text{m}$ )	Geometric surface area ( $\text{m}^2 \text{m}^{-3}$ )
	TiN-based ceramics <sup>a</sup>				
	Cotton-cloth/TiN	70–77	$2 \times 10^{-6}$	12	$12 \times 10^4$
	Cotton-wool/TiN	93–95	$70 \times 10^{-6}$	37	$3 \times 10^4$
<sup>a</sup> Number of pulses for PCVI treatment of TiN; 10,000	Filter paper/TiN	84–88	$9 \times 10^{-6}$	18	$8 \times 10^4$
	Wood/TiN	80–86	$7 \times 10^{-6}$	15	$18 \times 10^4$
<sup>b</sup> Volume fraction of active material layer per unit electrode volume	Foil-type current collector	(75) <sup>b</sup>	$<10^{-6}$	–	$1 \times 10^4$
	Metal-foam current collector	92–96	$<10^{-6}$	200	$3 \times 10^4$

In addition, open pore structure is needed for the application of porous ceramics to the current collector for the rechargeable batteries because the active materials of the battery are to fill into the pores of TiN ceramics. To decrease the resistivity with uniform infiltration of the stoichiometric TiN layer, the optimization of the CVI conditions is now open to further investigation.

Table 2 shows the properties of porous TiN-based ceramics as the current collector for the rechargeable batteries, along with these of the foil-type current collector for lithium-ion battery (LIB) and the metal (Ni)-foam current collector for Ni–Cd battery. In the commercial LIB, the volume fraction of the active materials' layer per unit volume of the electrode was estimated to be about 75% from simple geometric calculation [14]. Porosity (i.e. free space for filling with active materials) of each sample is higher than 75% except for the sample prepared from the carbonized cotton-cloth substrate. The apparent resistivities of the present samples are in the range of  $10^{-5}$  from  $10^{-6}$   $\Omega$  m. It is preferable to decrease the resistivity of the porous ceramics for the reduction of internal resistance of the electrode. As mentioned above, the optimization of the CVI conditions is now open to further investigation to reduce the resistivity of the deposited TiN film. The average pore sizes are below 40  $\mu\text{m}$ , which are lower than the thickness of the active materials' layer in the commercial LIB and the pore size of the metal (Ni)-foam current collector for Ni–Cd battery. Large cavity is unsuitable for LIB because of the low conductivity of the active materials and the electrolytes. The geometric surface area per unit volume of each porous TiN-based ceramic shows higher value than that of the conventional foil-type current collector, which would lead to the reduction of contacting resistance between active materials and current collectors. The sample obtained from the carbonized wood substrate has the highest surface area, therefore, it was expected that the contacting resistance became the lowest value in use of the TiN/wood porous bodies as current collector.

Galvanostatic cycling was applied at apparent current density of 0.3  $\text{mA cm}^{-2}$  in potential range from 0 to 3 V

vs.  $\text{Li/Li}^+$ . Under the present condition, TiN was inert against the electrochemical reaction with Li ion or electrolyte.

## Conclusions

In this study, the new preparation process of the electroconductive porous ceramics was investigated using PCVI of TiN into highly porous carbon substrates prepared by the carbonization of cotton, paper, and wood. And the properties on the current collector were estimated for the lithium-ion secondary batteries. Porous TiN-based ceramics having the three-dimensionally continuous current paths were obtained by the partial densification of the carbon substrates with TiN. Porosity of each sample is more than 80%, which was higher than the volume fraction of the active materials layer per unit volume of the electrode in the commercial lithium-ion battery. The apparent resistivity was rapidly lowered at the early stage of TiN infiltration and reached the value in the range of  $10^{-5}$ – $10^{-6}$   $\Omega$  m. The geometric surface area per unit volume of the sample was higher than that of the conventional foil-type current collector, which would lead to the reduction of contacting resistance between active materials and current collectors. The surface area showed the highest value for the sample obtained from carbonized wood substrate.

**Acknowledgement** The present work was partially supported by Grant-in-aids for Scientific Research from Ministry of Education, Culture, Sports, Science and Technology.

## References

- Golecki I (1997) Mater Sci Eng R 20:37
- Naslain R, Langlais F, Vignoles G, Pailler R (2007) Ceram Eng Sci Proc 27:373
- Naslain R (1992) J Alloy Compd 188:42
- Besmann TM, Stinton DP, Lowden RA, Probst KJ, Anderson TJ (2000) Ind Ceram 20:112
- Sugiyama K, Nakamura T (1987) J Mater Sci Lett 6:331

6. Langlais F, Dupel P, Pailler R (1996) In: Besmann TM, Allendorf MD, Robinson McD, Ulrich RK (eds) Proceedings of the 13th International Conference on CVD. Electrochemical Society, New Jersey, p 555
7. Jeong HJ, Park HD, Lee JD, Park JO (1996) Carbon 34:417
8. Ohzawa Y, Takahashi M, Sugiyama K (1997) J Mater Sci 32:4289
9. Sugiyama K, Ohzawa Y (1989) J Mater Sci 24:3756
10. Ofori JY, Sotirchos SV (1996) J Mater Res 11:2541
11. Ohzawa Y, Sakurai T, Sugiyama K (1999) J Mater Proc Tech 96:151
12. Ohzawa Y, Nakane K, Gupta V, Nakajima T (2002) J Mater Sci 37:2413
13. Komiyama H (1991) In: CVD handbook. Asakura Publishing, Tokyo, pp 572–584 (in Japanese)
14. Yoshio M, Ozawa S (2000) In: Lithium-ion secondary battery 2. Nikkan Kogyo Shinbun, Tokyo, pp 173–177 (in Japanese)